EXPERIMENTAL

H. Brodoefel
B. Klumpp
A. Reimann
M. Ohmer
M. Fenchel
S. Schroeder
S. Miller
C. Claussen
A. F. Kopp
A. M. Scheule

Late myocardial enhancement assessed by 64-MSCT in reperfused porcine myocardial infarction: diagnostic accuracy of low-dose CT protocols in comparison with magnetic resonance imaging

S. Schroeder
Department of Cardiology,
Eberhard-Karls-University,
Otfried-Müller-Str. 10,
72076 Tübingen, Germany

A. M. Scheule
Department of Thoracic,
Cardiac and Vascular Surgery,
Hoppe-Seyler-Str. 3,
72076 Tübingen, Germany

Abstract The purpose was to assess the practicability of low-dose CT imaging of late enhancement in acute infarction. Following temporary occlusion of the second diagonal branch, seven pigs were studied by multislice computed tomography (MSCT) and magnetic resonance imaging (MRI). Thus, 64-slice CT was performed at 3, 5, 10 and 15 min following the injection of contrast medium according to a bolus/low-flow protocol. Standard parameters of 120 kV and 800 mAs were compared with 80 kV and 400 mAs in various combinations. Infarct volumes were assessed as percentage of the ventricle for both MSCT and MR images. CT density values for viable and infarcted myocardium were obtained and image quality assessed. Mean infarct volume as measured by MRI was 12.33± 7.06%. MSCT achieved best correlation of volumes at 5 and 10 min. Whilst lowering of tube current resulted in poor correlation, tube voltage did not affect accuracy of infarct measurement (r^2=0.92 or 0.93 at 5 min, 800 mAs and 80 or 120 kV). In terms of image quality, greater image noise with 80 kV was compensated by significantly better contrast enhancement between viable and non-viable myocardium at lower voltage. Myocardial viability can accurately be assessed by MSCT at 80 kV, which ensures higher contrast for late enhancement and yields good correlation with MRI.

Keywords Multislice helical CT · Myocardial viability · Low-dose protocol

A.F. Kopp and A.M. Scheule contributed equally to this study

H. Brodoefel (✉) · B. Klumpp ·
A. Reimann · M. Ohmer · M. Fenchel ·
S. Miller · C. Claussen · A. F. Kopp
Department of Diagnostic Radiology,
Eberhard-Karls-University,
Hoppe-Seyler-Str. 3,
72076 Tübingen, Germany
e-mail: h.brodoefel@t-online.de
Tel.: +49-7071-2987212
Fax: +49-7071-295845

Introduction

In clinical routine, differentiation of viable from non-viable myocardium is crucial to predict functional recovery in the culprit arterial territory [1, 2].

So far, assessment of myocardial viability is performed only by single photon emission computed tomography (SPECT), positron emission tomography (PET), stress echocardiography or magnetic resonance imaging (MRI) [3–6].

The application of MRI for the diagnosis of ischemic heart disease has been subject of extensive studies and recently MRI has been shown to be superior to SPECT in the detection of very small infarcts [7–10]. In MRI, non-viable myocardium is revealed through the use of extracellular contrast agents, most notably Gd-DTPA, and the phenomenon of delayed myocardial enhancement (LE). The latter is non-specific, yet generally associated with a local enlargement of distribution volume for contrast material [11]. In the setting of acute myocardial infarction

(MI), LE is explained by myocyte necrosis, sarcomere membrane rupture and passive diffusion of contrast into the intracellular space [12, 13].

MRI excels at unmatched correlation with acute infarct size as well as excellent tissue contrast [14–17]. Yet, the technique is time-consuming and excludes not only the large collective of pacemaker patients but also those with acute and severe chest pain in whom aortic dissection or pulmonary embolism are on the differential to myocardial infarction.

Due to similar kinetics of extracellular contrast agents used for computed tomography (CT), the latter has the potential to visualise the LE phenomenon and early experience in animal models dates back to 1982 [18, 19]. However, until now both insufficient spatial and temporal resolution of single-slice CT and concerns about increasing X-ray exposure with additional late scans have prevented the widespread use of CT for this application. Hence, so far infarct detection by multislice CT (MSCT) has most often been based on the description of early perfusion deficits. The latter correlate well with infarct size in non-reperfused MI [20, 21]. In the setting of reperfusion, however, MSCT first pass imaging shows poor accuracy and significant underestimation of infarct size [22, 23].

With the advent of new generation detectors, direct assessment of myocardial viability by means of late enhancement MSCT has evoked increasing interest and initial results are very promising [22, 24–28]. Nevertheless, there is still no consensus concerning the best suitable CT protocols for imaging LE. Above all, there is lack of agreement concerning the radiation dose required for accurate image quality. Whilst most studies have been performed with standard 120 kV and 800 mAs full-dose protocols, there are also promising results with lower dose late-phase CT scans [22, 26, 27].

However, in the process of establishing MSCT in routine assessment of viability the question of radiation dose is a major issue.

Thus the aim of this study was to evaluate the practicability of low-dose late-phase imaging of acute infarction through systematic evaluation of variable dose protocols in comparison with MRI.

Materials and methods

Open-heart surgery was performed in ten German farm pigs (mean weight: 46±3.28 kg). The procedures and animal care conformed to the "Guide for the Care and Use of Laboratory Animals" (National Institutes of Health; publication no. 86–23, revised 1985) and the German Law on the Protection of Animals.

Following intramuscular pre-medication (0.05 mg atropine; 4 mg azaperone; 1 mg diazepame and 7 mg/kg of bodyweight ketamine), anaesthesia was induced (0.05 mg fentanyl and 3 mg/kg of bodyweight propofole). Animals were intubated and mechanically ventilated with gas anaesthesia (1.5% isoflurane). Analgesia was achieved by fentanyl 0.03 mg/kg/h during operation and buprenorphine or carprofene postoperatively. The entire operation was performed with ECG monitoring and multiple blood gas analysis. Xylocaine (3 mg/kg/h) was administered to prevent ventricular fibrillation.

After left antero-lateral thoracotomy was performed, the pericardium was opened and the second diagonal branch of the left anterior descending artery was temporarily ligated for 90 min. After reopening the diagonal branch a 10-min period of ventricular tachycardia and arrhythmia was followed and treated by increasing the xylocaine dose (6 mg/kg/h). Subsequently, pericardium and thoracotomy were closed without placing a chest tube.

Two animals showed ventricular fibrillation when the pericardium was opened, both were successfully defibrillated. Three animals died as the result of persistent fibrillation: two 30 and 60 min after induction of infarctionand one during reperfusion.

Animals were imaged a median 1 day post infarction (one 2 days, one 4 days post MI). Following pre-medication, anaesthesia was achieved with pentobarbital 25 mg/kg of bodyweight; the pigs were intubated and ventilated both mechanically during CT and manually during MRI examination. Images were obtained during repeated breath holds.

Retrospectively ECG-gated MSCT was performed prior to MRI imaging in the supine position, using a 64-slice scanner (Somatom, Sensation 64, Siemens Medical Systems, Forchheim, Germany). Average heart beat was 72 beats per min (bpm).

A total of 1.5 ml/kg of bodyweight highly concentrated contrast agent iomeprol (Iomeron 400, Altana) was intravenously administered according to the following protocol: the total amount of contrast minus 30 ml was injected as a bolus (3–4 ml/s), 30 ml were applied over approximately 5 min, starting 60 s after the initial bolus application and running at low rate of 0.1 ml/s. For all CT examinations a standard protocol was used: collimation 64×0.6 mm, gantry rotation time 330 ms, pitch 0.23.

CT examinations were obtained 3, 5, 10 and 15 min after initial contrast application. At 3 and 10 min, a tube voltage of 80 kV along with both the standard 800 mAs for 64-MSCT and a lower tube current of 400 mAs were used. At 5 min, four scans were obtained with all combinations of standard 120 kV and 800 mAs or 80 kV and 400 mAs. The final scan at 15 min was obtained using 80 kV and 800 mAs.

Axial images with an effective slice thickness of 1.0 mm and a reconstruction increment of 0.6 mm were reconstructed at 60% of the RR-interval. In the very rare cases of motion artefacts additional preview-series were obtained, assessed for artefacts in 5% increments and used to orientate improved reconstruction intervals.

For further analysis short axis multiplanar reformats [5-mm thick mutiplanar reconstructions (MPRs), no gap] were calculated.

Radiation dose was calculated using CT-Expo V 1.5 (Drs. Nagel and Stamm, Germany).

All MRI studies were performed with a 1.5-Tesla MR scanner (Magnetom Sonata; Siemens, Erlangen, Germany) using a phased-array body coil. For assessment of myocardial viability, 5-mm short axis slices without gap were obtained 15 min post injection of 0.2 mmol/kg of bodyweight Gd-DTPA (Magnevist, Schering) and using a ECG-triggered, segmented inversion recovery prepared turbo FLASH sequence (TR 9.56 ms, TE 4.38 ms, flip angle 25°, two averages, 25 lines per segment, voxel size 1.25×2.5×5.0 mm). Optimal inversion time (TI) was determined using a TI scout in order to minimise signal in normal myocardium.

On an offline workstation (Leonardo, Siemens), CT and MR images were assessed by separate readers blinded to the results of the other imaging technique (H.B. and B.K.). For quantification of infarct volumes, both endo- and epicardial contours of the left ventricle as well as contours of late enhancement were manually drawn on 5-mm MRI or MSCT sections. Myocardial volume was then calculated by subtraction of endocardial from epicardial area with the remainder being multiplied by section thickness. Volumes of late enhancement were likewise assessed through multiplication of area with section thickness and fractional infarcted myocardium was calculated in terms of percentage of left ventricular volume.

CT density values of late enhancement, viable myocardium and left ventricular cavity were measured for all time points at 80 kV and 800 mAs, at 5 min additionally at 120 kV and 800 mAs.

For all time-points and scanning parameters, quality of MSCT LE images was graded by two radiologists (H.B. and A.R.) as follows: 1, excellent (good delineation of infarcted myocardium in all parts); 2, good (good delineation of infarcted myocardium in most parts); 3, poor (loss of clear delineation in all parts); 4, very poor (no visibility or merely diagnosis of LE). Agreement between readers was examined by weighted *kappa* statistics. Discordant readings were resolved by consensus between the two readers.

Statistical analysis was performed with software (GraphPad Prism version 4.00, San Diego, Calif.). Data are expressed as mean±standard deviation (SD) for continuous variables and as frequencies or percentages for categorical variables. A P value of less than 0.05 indicated statistical significance.

Results

Mean infarct volume as measured by MRI was 12.33± 7.06%. Comparison of infarct zones with MSCT revealed best correlation at 5 and 10 min after initial contrast injection and use of 80 or 120 kV with 800 mAs (Table 1). With these time-points and scanning parameters, MSCT showed slight over-estimation of infarct area when compared with MRI (Fig. 1).

Volumes of LE proved time-dependent and there was a significant rise of infarct area during 3 and 15 min, most of which occurred within the first 5 min (P=0.040; repeated measures ANOVA with Tukey's post test for all time-points at 80 kV and 800 mAs).

At 3, 5 and 10 min, infarct volumes were assessed at both 400 and 800 mAs. For these time-points, lowering of the tube current at 80 kV resulted in greater image noise with under-estimation of infarct size in comparison with higher tube current (P=0.20; 0.26 and 0.11; paired t-tests) and weaker correlation with MRI.

On the other hand, at 5 min, lowering of the tube voltage from 120 to 80 kV at 800 mAs would not affect precision of

Table 1 Correlation of MI size between MRI and MSCT at various time-points and dose applications

Time	Voltage	Current	Pearson correlation coefficient	r^2
3 min	80 kV	400 mAs	0.79 (CI 0.096–0.96)	0.62
		800 mAs	0.91 (CI 0.52–0.98)	0.83
5 min	80 kV	400 mAs	0.82 (CI 0.19–0.97)	0.68
		800 mAs	0.96 (CI 0.75–0.99)	0.92
	120 kV	400 mAs	0.80 (CI 0.12–0.96)	0.64
		800 mAs	0.97 (CI 0.79–0.99)	0.93
10 min	80 kV	400 mAs	0.85 (CI 0.29–0.97)	0.73
		800 mAs	0.96 (CI 0.79–0.99)	0.93
15 min	80 kV	800 mAs	0.92 (CI 0.58–0.98)	0.86

Fig. 1 MI size in percent of the left ventricle as measured by MRI or MSCT at various time-points and application of variable tube voltage or current. The first number indicates time (min); the second, tube voltage and current
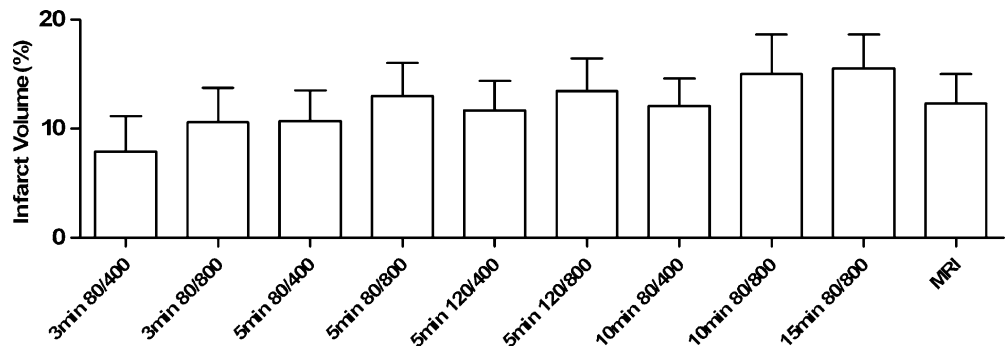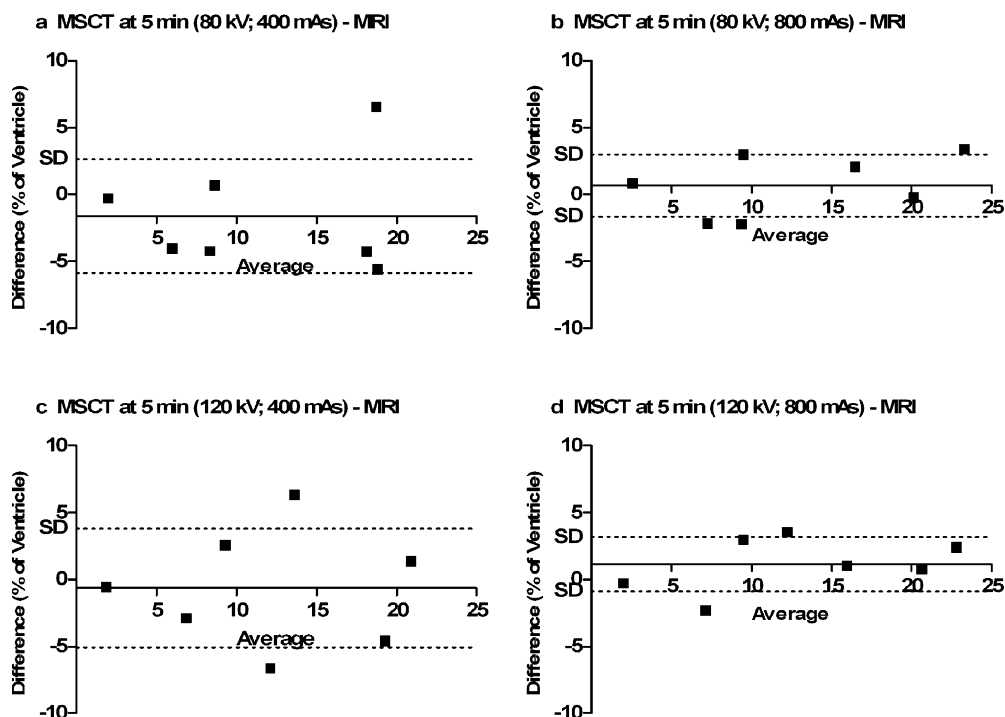
Fig. 2 Bland-Altman plots comparing MI size between MRI and MSCT at 5 min and variable dose application. The *x*-axis denotes the average of MSCT and MRI, the point of intersection with the *y*-axis indicates the bias of MSCT. *Dotted lines* show the standard deviation of the bias

volume estimation. In Fig. 2, Bland-Altman plots are provided for scans obtained at 5 min and various dose protocols. Estimations of radiation dosages with use of various protocols are provided in Table 2.

For lower 80 kV tube voltage (800 mAs) results of quantitative analysis of CT attenuation in zones of LE, viable myocardium and the left ventricular cavity are presented in Fig. 3a. At 80 kV, the HU contrast between LE and normal myocardium proved significant for each time-point ($P<0.001$; repeated measures ANOVA with Tukey's post test) and showed an increase from 50.4±8.7 or 51.7±8.4 HU at 3 or 5 min to 64.1±9.7 or 63.7±12.0 HU at 10 or 15 min. The HU contrast between LE and the left ventricular cavity was significant only for 3 and 5 min ($P<0.01$; repeated measures ANOVA with Tukey's post test).

As evident from Fig. 3b, with 120 kV (800 mAs) the HU contrasts between cardiac structures were less marked when compared with lower voltage. In fact, at 5 min, when both 80 and 120 kV images were obtained, the difference between HU of LE and viable myocardium was significantly reduced from 51.7 HU at 80 kV to 31.6 HU at 120 kV tube voltage ($P=0.0003$; paired *t*-test). Also, at 5 min use of 120 kV would achieve no significant contrast between LE and left ventricular cavity.

This rise in contrast with use of 80 kV is reflected by the evaluation of image quality according to the criteria explained above (Fig. 4). Inter-rater agreement in the evaluation of image quality was good (weighted *kappa*=0.72). High contrast between LE, viable myocardium and left ventricular cavity explains best image quality at 5 or 10 min and use of 80 kV and 800 mAs (Figs. 5, 6 and 7).

Discussion

In the setting of ischemic heart disease with severe left ventricular dysfunction, detection of residual myocardial viability is of great importance for the planning of therapeutic strategy.

MRI is well established for this application, yet with regard to numerous contraindications, the advance of dual-phase MSCT seems reasonable. This is because since CT shows unmatched quality in imaging coronary arteries and has the additional ability to assess left ventricular function [29–31].
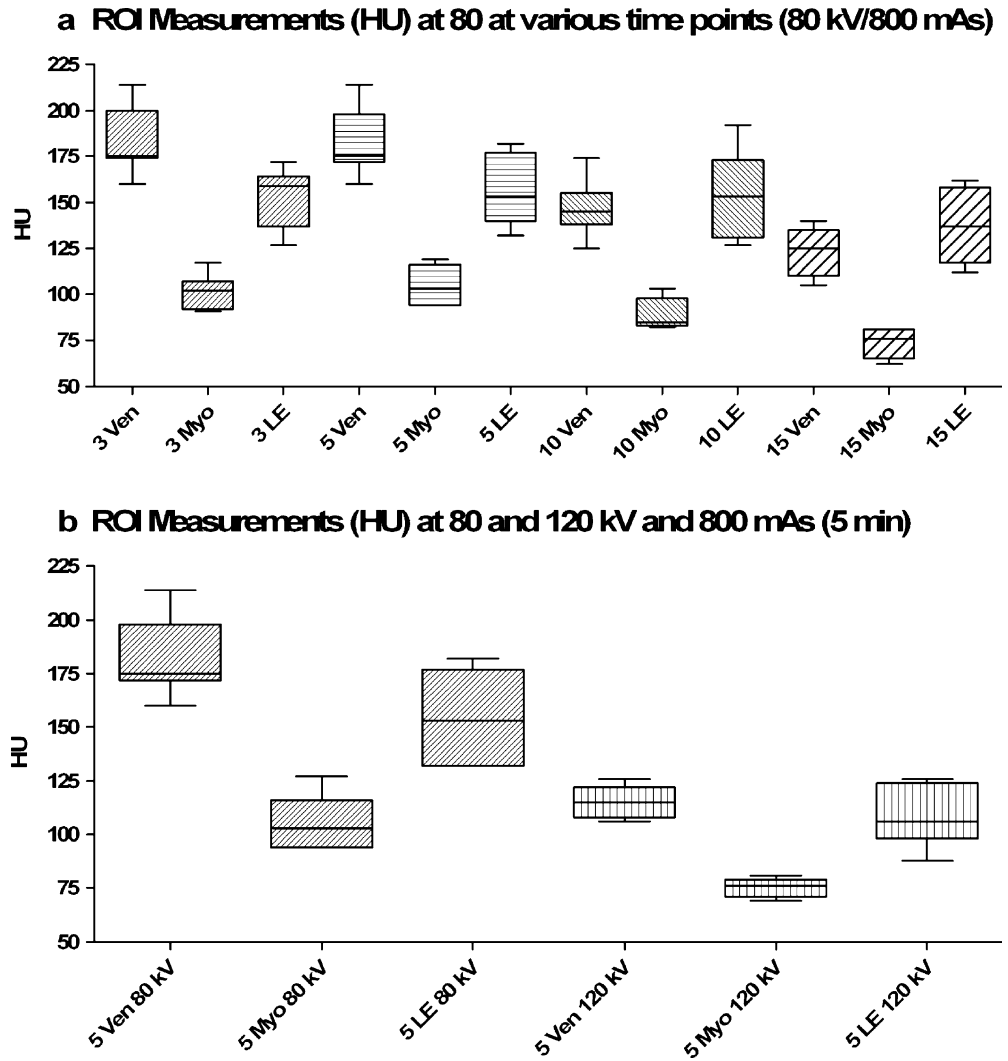
First results with new generation MSCT scanners are promising. Still, until now there is no agreement concerning the most suitable dual-phase CT protocol. Above all, dose remains an important issue and will have a great impact on the long-term adoption of MSCT for assessment of myocardial viability.

Using a bolus/low-flow contrast protocol, a good match of LE in MRI and MSCT was achieved in our study, whilst direct comparison of 120 kV and 80 kV would show no

Table 2 Estimation of radiation dose at variable scanning parameters

Tube voltage	Tube current	Effective dose (mSv)	Dose-length product (mGy×cm)
80 kV	400 mAs	2.8	166
	800 mAs	5.7	333
120 kV	400 mAs	7.8	459
	800 mAs	15.6	917

Fig. 3a, b CT density values for late enhancement (*LE*), viable myocardium (*Myo*) and ventricular cavity (*Ven*). **a** HU at various time-points and constant application of 80 kV and 800 mAs. **b** presents HU at 5 min, comparing 80 kV with 120 kV at 800 mAs

a ROI Measurements (HU) at 80 at various time points (80 kV/800 mAs)

## b ROI Measurements (HU) at 80 and 120 kV and 800 mAs (5 min)

advantage of higher tube voltage. On the contrary, whilst for both protocols there was no difference in correlation of LE with MRI, a significantly higher contrast between left ventricular cavity, viable myocardium and LE more than compensated for elevated image noise at 80 kV and led to slightly better image quality with use of a low-dose protocol. At the same time, we showed that reduction of tube current leads to an unacceptable increase of image noise, which has a considerable effect on both estimation of infarct area and image quality.

Apart from the obvious benefit of dose reduction, there is a technical rationale to lower tube voltage. Due to the

Fig. 4 Image quality, as defined above, at variable time-points and dose applications. The first number indicates time, the second tube voltage and current
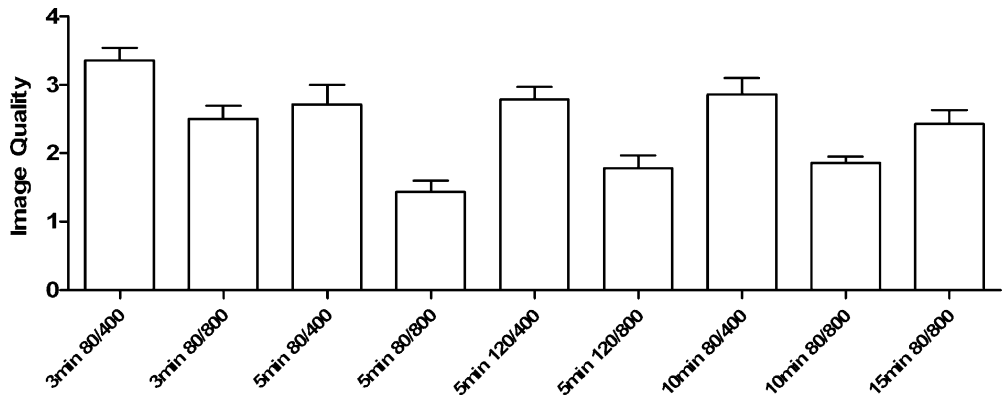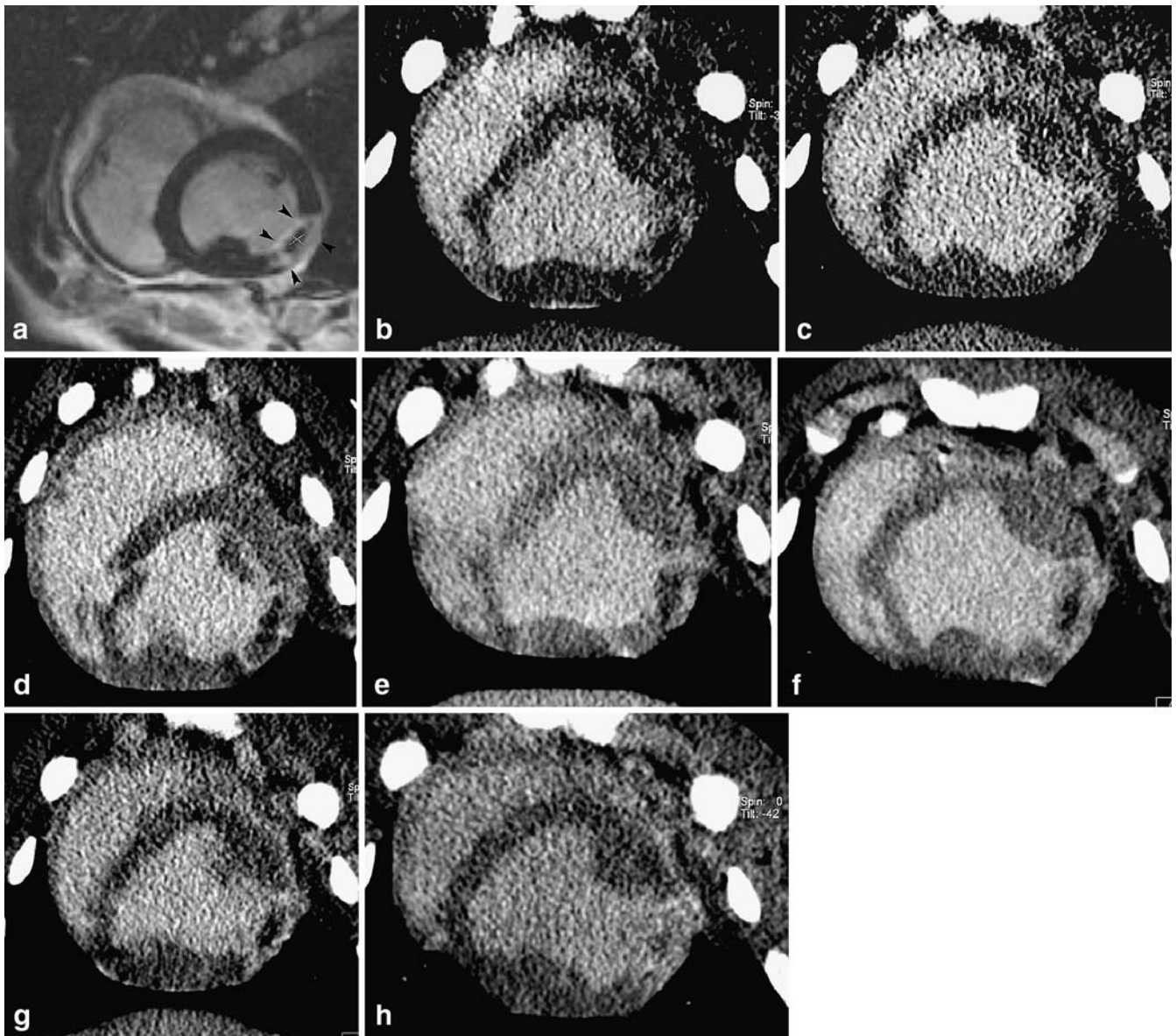
Fig. 5a–h MR and MSCT images of a transmural antero-lateral infarction. **a** On the MR image, *arrows* indicate the zone of late enhancement. The low signal area at the centre of infarcted tissue (*cross*) corresponds to areas of "no-reflow", caused by microvascular obstruction in the setting of reperfusion. MSCT images are shown **b** at 3 min with 80 kV/800 mAs, **c** at 5 min with 80 kV/400 mAs, **d** 80 kV/800 mAs, **e** 120 kV/400 mAs and **f** 120 kV/800 mAs. Scans **g** and **h** were obtained at 10 and 15 min with 80 kV/800 mAs each. Images show good correlation with MRI contrast phenomena, whilst LE volume increases over time. Comparing 80 with 120 kV, the latter reduces image noise with no gain in image quality due to better contrast at 80 kV. Reduction of current, on the other hand, degrades image quality through increase of image noise. At 5 min, HU for blood, viable myocardium and LE were 165, 97 and 135 at 80 kV or 108, 70 and 96 at 120 kV

high atomic number of iodine, a tube voltage of 80 kV achieves a more optimal absorption of radiation and hence allows for better contrast enhancement. In fact, through use of 80 kV (800 mAs) for late phase scans dose is lowered by 65% when compared with standard acquisition parameters [32]. However, increase of contrast at low-dose scanning comes at the cost of greater image noise. In fact, using 80 kV, the latter was shown to exponentially increase in thoracic imaging of patients weighing more than 75 kg [32]. Nevertheless, using low-dose 80 or 90 kV protocols, assessment of myocardial viability has repeatedly been performed with good results in humans, notably in 34 consecutive patients by Paul et al. [26], 37 patients by Gerber et al.[33] and 28 patients weighing 80.6±15.7 kg by Mahnken et al. [22]. Eventually, however, weight issues remain a considerable limitation to the exclusive use of low kilovoltage protocols in clinical routine.

Fig. 6 a MRI showing a transmural antero-lateral infarction with both zones of late enhancement (*arrows*) and "no-reflow" (*cross*). **d** In this example, best CT image quality is provided at 5 min and use of 80 kV/800 mAs. **f** Application of 120 kV/800 mAs slightly reduces image noise at the cost of contrast between tissues. **c, e** At both 80 kV and 120 kV, lowering of tube current to 400 mAs leads to strong increase of image noise and deterioration of image quality. At 5 min HU for blood, viable myocardium and LE were 214, 122 and 182 at 80 kV or 123, 80 and 126 at 120 kV. **b** At 3 min 80 kV/800 mAs, there is incomplete enhancement of the infarct zone with dominance of the "no-reflow" area. **g** At 15 min 80 kV/800 mAs, there is still considerable contrast to non-viable myocardium. However, washout with low contrast to viable myocardium and blood results in poor delineation of cardiac structures and degradation of image quality
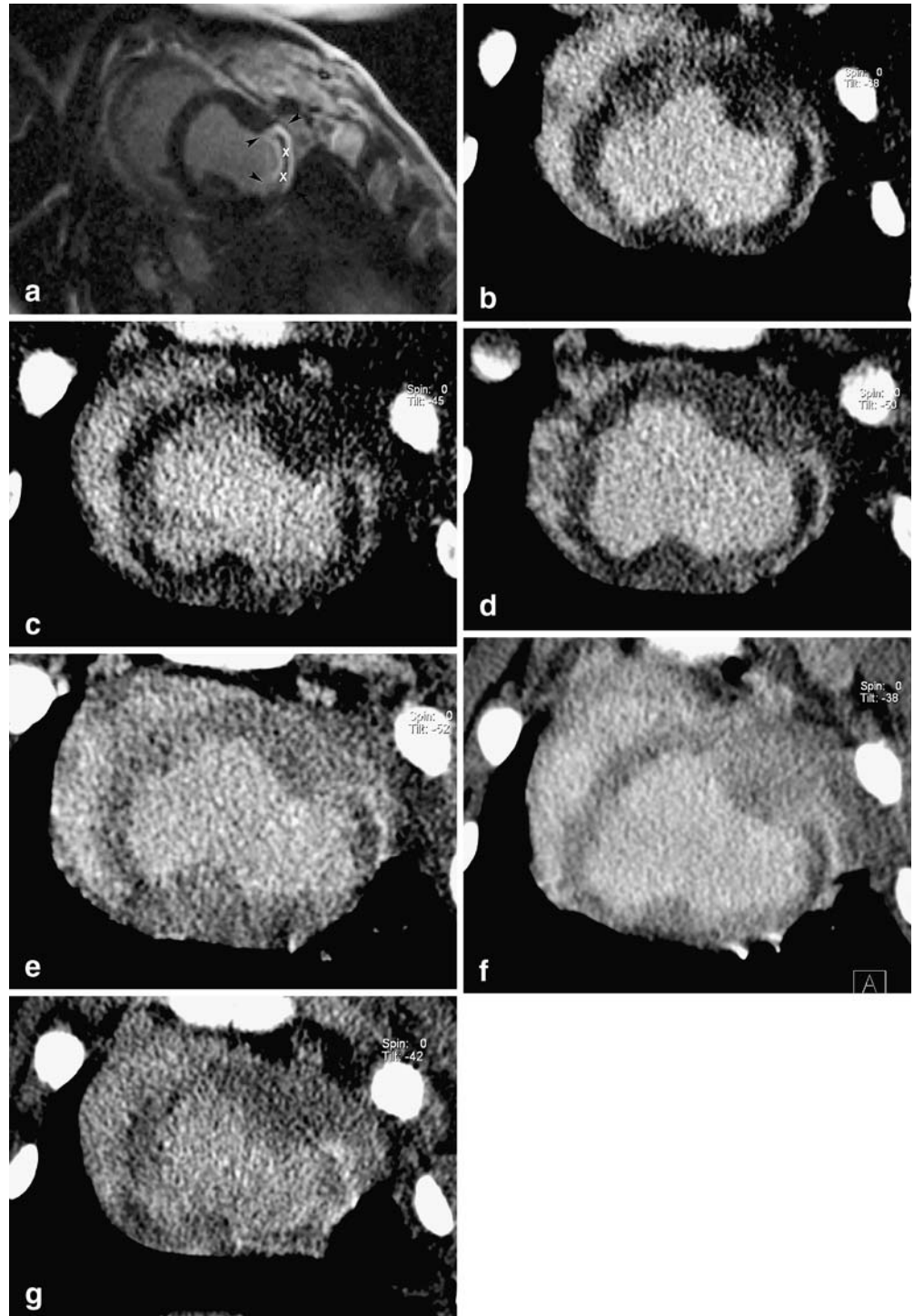
Of note, in our study, good image quality and correlation was obtained with the use of a bolus/low-flow rather than a pure bolus contrast protocol. It is known from dynamic MRI studies that delivery of contrast material to the non-viable tissue is a time dependent process which may not be completed prior to 5 min [10, 34, 35]. On the other hand, with MSCT excessive fading of contrast from blood and normal myocardium is a major problem and degrades overall image quality, even though absolute contrast to the LE zone may still be considerable. With application of a single bolus, however, clearing of contrast from blood pool and tissue occurs early and concomitant to ongoing distribution of contrast agent in the infarct zone. This is especially true when moderate contrast doses are used.
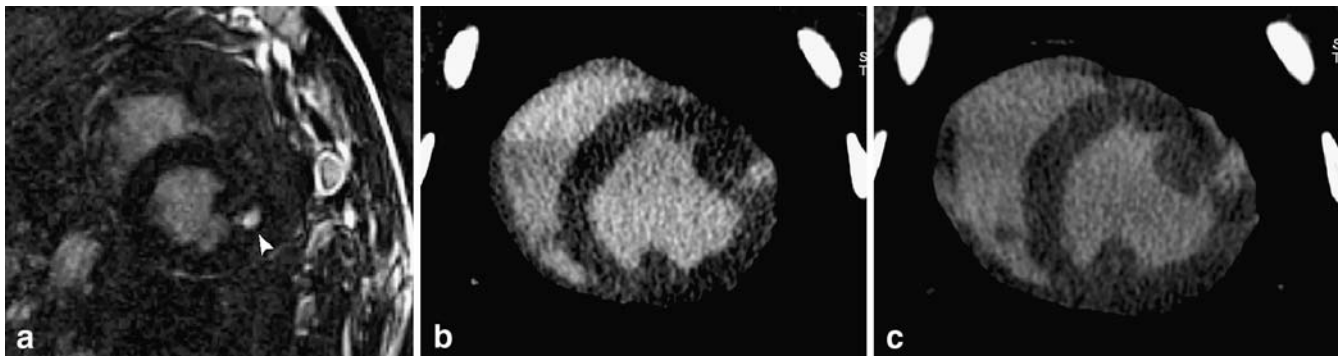
Fig. 7 a MRI showing a small non-transmural subepicardial infarction (*arrow*). MSCT images at 5 min, 80 (**b**) or 120 kV (**c**) and 800 mAs are shown at the same window level and width of 190/170. HU for blood, viable myocardium and LE were 203, 101 and 180 at 80 kV or 126, 76 and 122 at 120 kV

Thus, the primary advantage of a several minutes low-grade inflow lies with persistent delivery of contrast to non-pathological cardiac tissue and blood. Particularly, in our study, this ongoing inflow resulted in a significant HU difference between blood pool and LE at 3 and 5 min and use of 80 kV.

Such significant HU contrast, however, allows better differentiation of cavity from infarct zone and may be especially helpful in the absence of associated "no-reflow" phenomenon. The latter is caused by microvascular obstruction in the setting of reperfusion and leads to reduced contrast delivery in the subendocardium of acute MI. If present marked subendocardial hypoenhancement in the "no-reflow" zone may greatly facilitate the delineation of cavity in late MSCT imaging.

In our study, MSCT volumes of LE showed a significant increase over time, most of which occurred within the first 5 min. From MRI studies, it is known that imaging too early (e.g. <5 min) may result in underestimation of infarct region [36]. This time dependence of infarct area presumably reflects progressive distribution of contrast in infarcted tissue and has also been reported for late enhancement MSCT [22]. Due to the use of a continuous low-flow contrast supply this process was most likely accentuated in our study.

In our model, best image quality and correlation with MRI was achieved at 5 and 10 min after initial contrast application. At 3 min, contrast distribution within the infarct zone was still incomplete, and at 15 min, progres-sive washout led to considerable deterioration of image quality. Our findings regarding the most suitable time points for late scan imaging are in line with results from recent animal studies, which all favour 5 or 10 min as optimal delay with peak intensity of LE [22, 27, 28, 37].

The comparatively small number of animals is an obvious limitation to this pilot study. The adjustment of the window centre was not fully standardised but rather oriented by subjective definition of optimal contrast.

As discussed above, the use of a bolus/low-flow contrast protocol is a technical issue leading to distinct contrast kinetics that differ from the pure bolus protocols which most groups have used so far. This does, however, not affect the primary finding of this study, namely the feasibility of low-dose late-scan MSCT.

In summary, our study demonstrates that in an animal model use of a low dose 80 kV late-phase protocol leads to higher tissue contrast, which compensates for the increase of image noise and allows good correlation with LE in MRI. At this stage, the latter is certainly more robust and provides better image quality. With use of low-dose scanning protocols, however, MSCT becomes more competitive in the assessment of myocardial viability and larger studies seem warranted to establish MSCT as an alternative in case of contraindications to MRI.

References

1. Beek AM, Kuhl HP, Bondarenko O et al (2003) Delayed contrast-enhanced magnetic resonance imaging for the prediction of regional functional improvement after acute myocardial infarction. J Am Coll Cardiol 42:895–901

2. Gutberlet M, Frohlich M, Mehl S et al (2005) Myocardial viability assessment in patients with highly impaired left ventricular function: comparison of delayed enhancement, dobutamine stress MRI, end-diastolic wall thick-ness, and TI201-SPECT with functional recovery after revascularization. Eur Radiol 15:872–880

3. Burt RW, Perkins OW, Oppenheim BE et al (1995) Direct comparison of fluorine-18-FDG SPECT, fluorine-18-FDG PET and rest thallium-201 SPECT for detection of myocardial viability. J Nucl Med 36:176–179

4. Mahrholdt H, Wagner A, Judd RM, Sechtem U (2002) Assessment of myocardial viability by cardiovascular magnetic resonance imaging. Eur Heart J 23:602–619

5. Brunken R, Tillisch J, Schwaiger M et al (1986) Regional perfusion, glucose metabolism, and wall motion in patients with chronic electrocardiographic Q wave infarctions: evidence for persistence of viable tissue in some infarct regions by positron emission tomography. Circulation 73:951–963

6. Sicari R, Picano E, Landi P et al (1997) Prognostic value of dobutamine-atropine stress echocardiography early after acute myocardial infarction. Echo Dobutamine International Cooperative (EDIC) Study. J Am Coll Cardiol 29:254–260

7. Wagner A, Mahrholdt H, Holly TA et al (2003) Contrast-enhanced MRI and routine single photon emission computed tomography (SPECT) perfusion imaging for detection of subendocardial myocardial infarcts: an imaging study. Lancet 361:374–379

8. Pereira RS, Prato FS, Wisenberg G, Sykes J (1996) The determination of myocardial viability using Gd-DTPA in a canine model of acute myocardial ischemia and reperfusion. Magn Reson Med 36:684–693

9. McNamara MT, Tscholakoff D, Revel D et al (1986) Differentiation of reversible and irreversible myocardial injury by MR imaging with and without gadolinium-DTPA. Radiology 158:765–769

10. Kim RJ, Fieno DS, Parrish TB et al (1999) Relationship of MRI delayed contrast enhancement to irreversible injury, infarct age, and contractile function. Circulation 100:1992–2002

11. Hillenbrand HB, Kim RJ, Parker MA, Fieno DS, Judd RM (2000) Early assessment of myocardial salvage by contrast-enhanced magnetic resonance imaging. Circulation 102:1678–1683

12. Flacke SJ, Fischer SE, Lorenz CH (2001) Measurement of the gadopentetate dimeglumine partition coefficient in human myocardium in vivo: normal distribution and elevation in acute and chronic infarction. Radiology 218:703–710

13. Kim RJ, Chen EL, Lima JA, Judd RM (1996) Myocardial Gd-DTPA kinetics determine MRI contrast enhancement and reflect the extent and severity of myocardial injury after acute reperfused infarction. Circulation 94:3318–3326

14. Thomson LE, Kim RJ, Judd RM (2004) Magnetic resonance imaging for the assessment of myocardial viability. J Magn Reson Imaging 19:771–788

15. Simonetti OP, Kim RJ, Fieno DS et al (2001) An improved MR imaging technique for the visualization of myocardial infarction. Radiology 218:215–223

16. Constantine G, Shan K, Flamm SD, Sivananthan MU (2004) Role of MRI in clinical cardiology. Lancet 363:2162–2171

17. Comte A, Lalande A, Walker PM et al (2004) Visual estimation of the global myocardial extent of hyperenhancement on delayed contrast-enhanced MRI. Eur Radiol 14:2182–2187

18. Huber DJ, Lapray JF, Hessel SJ (1981) In vivo evaluation of experimental myocardial infarcts by ungated computed tomography. AJR Am J Roentgenol 136:469–473

19. Slutsky RA, Mattrey RF, Long SA, Higgins CB (1983) In vivo estimation of myocardial infarct size and left ventricular function by prospectively gated computerized transmission tomography. Circulation 67:759–765

20. Hoffmann U, Millea R, Enzweiler C et al (2004) Acute myocardial infarction: contrast-enhanced multi-detector row CT in a porcine model. Radiology 231:697–701

21. Mahnken AH, Bruners P, Katoh M, Wildberger JE, Gunther RW, Buecker A (2006) Dynamic multi-section CT imaging in acute myocardial infarction: preliminary animal experience. Eur Radiol 16:746–752

22. Mahnken AH, Koos R, Katoh M et al (2005) Assessment of myocardial viability in reperfused acute myocardial infarction using 16-slice computed tomography in comparison to magnetic resonance imaging. J Am Coll Cardiol 45:2042–2047

23. Nikolaou K, Knez A, Sagmeister S et al (2004) Assessment of myocardial infarctions using multidetector-row computed tomography. J Comput Assist Tomogr 28:286–292

24. Koyama Y, Matsuoka H, Mochizuki T et al (2005) Assessment of reperfused acute myocardial infarction with two-phase contrast-enhanced helical CT: prediction of left ventricular function and wall thickness. Radiology 235:804–811

25. Koyama Y, Mochizuki T, Higaki J (2004) Computed tomography assessment of myocardial perfusion, viability, and function. J Magn Reson Imaging 19:800–815

26. Paul JF, Wartski M, Caussin C et al (2005) Late defect on delayed contrast-enhanced multi-detector row CT scans in the prediction of SPECT infarct size after reperfused acute myocardial infarction: initial experience. Radiology 236:485–489

27. Gerber BL, Belge B, Legros GJ et al (2006) Characterization of acute and chronic myocardial infarcts by multidetector computed tomography: comparison with contrast-enhanced magnetic resonance. Circulation 113:823–833

28. Lardo AC, Cordeiro MA, Silva C et al (2006) Contrast-enhanced multidetector computed tomography viability imaging after myocardial infarction: characterization of myocyte death, microvascular obstruction, and chronic scar. Circulation 113:394–404

29. Kopp AF, Kuttner A, Trabold T, Heuschmid M, Schroder S, Claussen CD (2003) Contrast-enhanced MDCT of the thorax. Eur Radiol 13(Suppl 3): N44–N49

30. Dirksen MS, Bax JJ, de Roos A et al (2004) Images in cardiovascular medicine. Dynamic multislice computed tomography of left ventricular function. Circulation 109:e25–e26

31. Kuettner A, Kopp AF, Schroeder S et al (2004) Diagnostic accuracy of multidetector computed tomography coronary angiography in patients with angiographically proven coronary artery disease. J Am Coll Cardiol 43:831–839

32. Sigal-Cinqualbre AB, Hennequin R, Abada HT, Chen X, Paul JF (2004) Low-kilovoltage multi-detector row chest CT in adults: feasibility and effect on image quality and iodine dose. Radiology 231:169–174

33. Gerber BL, Rochitte CE, Melin JA et al (2000) Microvascular obstruction and left ventricular remodeling early after acute myocardial infarction. Circulation 101:2734–2741

34. Saeed M, Lund G, Wendland MF, Bremerich J, Weinmann H, Higgins CB (2001) Magnetic resonance characterization of the peri-infarction zone of reperfused myocardial infarction with necrosis-specific and extracellular non-specific contrast media. Circulation 103:871–876

35. Weinmann HJ, Brasch RC, Press WR, Wesbey GE (1984) Characteristics of gadolinium-DTPA complex: a potential NMR contrast agent. AJR Am J Roentgenol 142:619–624

36. Edelman RR (2004) Contrast-enhanced MR imaging of the heart: overview of the literature. Radiology 232:653–668

37. Park JM, Choe YH, Chang S et al (2004) Usefulness of multidetector-row CT in the evaluation of reperfused myocardial infarction in a rabbit model. Korean J Radiol 5:19–24